Stem Cell Reports
Article

ISSCR

OPEN ACCESS

β Cell Replacement after Gene Editing of a Neonatal Diabetes-Causing Mutation at the Insulin Locus

Shuangyu Ma,[1] Ryan Viola,[1] Lina Sui,[1] Valentino Cherubini,[2] Fabrizio Barbetti,[3] and Dieter Egli[1,*]
[1]Naomi Berrie Diabetes Center & Department of Pediatrics, College of Physicians and Surgeons, Columbia University Medical Center, New York, NY 10032, USA
[2]Salesi Hospital, 60123 Ancona, Italy
[3]Bambino Gesù Children's Hospital, 00164 Rome, Italy
*Correspondence: de2220@cumc.columbia.edu
https://doi.org/10.1016/j.stemcr.2018.11.006

SUMMARY

Permanent neonatal diabetes mellitus (PNDM) can be caused by insulin mutations. We generated induced pluripotent stem cells from fibroblasts of a patient with PNDM and undetectable insulin at birth due to a homozygous mutation in the translation start site of the insulin gene. Differentiation of mutant cells resulted in insulin-negative endocrine stem cells expressing MAFA, NKX6.1, and chromogranin A. Correction of the mutation in stem cells and differentiation to pancreatic endocrine cells restored insulin production and insulin secretion to levels comparable to those of wild-type cells. Grafting of corrected cells into mice, followed by ablating mouse β cells using streptozotocin, resulted in normal glucose homeostasis, including at night, and the stem cell-derived grafts adapted insulin secretion to metabolic changes. Our study provides proof of principle for the generation of genetically corrected cells autologous to a patient with non-autoimmune insulin-dependent diabetes. These cases should be readily amenable to autologous cell therapy.

INTRODUCTION

Stem cell-derived pancreatic endocrine cells may be useful for replacing β cells lost due to the progression of insulin-dependent diabetes, in particular, in type 1 diabetes (T1D). A major challenge in developing cell replacement for T1D is the likely recurrence of autoimmunity and immune rejection of a heterologous cell product. The risks associated with immune suppression to avoid rejection outweigh the risks of continued disease management for most patients. Therefore, efforts have focused on the development of encapsulation methods to protect the graft from the immune system (Agulnick et al., 2015; Vegas et al., 2016). However, it is unclear if encapsulation can establish lasting independence from insulin therapy or will require repeated replacement of the cell device. All tissues require a connection to the vasculature for tissue turnover and clearance of cell debris, and β cells require high oxygen tension (Sato et al., 2011) and are in extensive contact with the vasculature (Bonner-Weir and Orci, 1982). Therefore, there is a rationale to evaluate the feasibility of β cell replacement without encapsulation. Because antigen-specific therapies to prevent recurrence of autoimmunity in T1D are not yet established, non-immune-mediated forms of diabetes might provide a suitable initial target for cell replacement. Monogenetic forms of diabetes are not caused by immune rejection, and can present with a phenotype identical to T1D, including dependence on exogenous insulin injections. Because monogenetic diabetes is caused by a defined genetic lesion, a combination of gene and cell therapy should be effective in restoring glucose homeostasis upon transplantation.

Here we report the identification of a point mutation in the start codon of the insulin locus ($INS^{ATG>ATA}$) in an individual patient with permanent neonatal diabetes mellitus (PNDM), and the correction of the mutation in induced pluripotent stem cells (iPSCs). Pancreatic endocrine cells differentiated from the stem cells with the mutation expressed markers of β cells and insulin mRNA, but did not contain or secrete insulin protein. Upon genetic correction of the mutation using CRISPR/Cas9 in iPSCs, corrected cells differentiated to pancreatic endocrine cells that produced insulin at levels indistinguishable from embryonic stem cell (ESC)-derived cells (wild-type controls). Grafting of gene-corrected endocrine cells into mice resulted in the secretion of detectable levels of human C-peptide in mouse serum. This was not observed when transplanting the uncorrected patient cells. Once endogenous mouse β cells were ablated using streptozotocin (STZ), corrected endocrine cells were able to maintain normoglycemia, while mice with mutant cells became diabetic. This demonstrates the potential to combine gene with cell therapy for diabetes, and provides a path toward restoring glucose homeostasis in patients with PNDM due to insulin gene mutations and, in general, in monogenetic forms of diabetes.

RESULTS

Clinical Features of Diabetes due to a Homozygous Mutation in the Start Codon of the Insulin Gene

The propositus, the son of consanguineous parents (first cousins), was delivered at the 37th week of gestation with

a weight of 1800 g. He initially presented with non-syndromic diabetes (fasting plasma glucose: 15.9 mmol/L) on the fifth day of life, without any detectible serum levels of C-peptide. The patient was placed on intravenous insulin therapy (0.05 UI/kg/hr), with substantial improvement of glucose levels within 9 days from treatment start. The subject was negative for autoantibodies in serum (i.e., ICA, GAD65, IA-2A, IAA) typical of T1D at diagnosis of diabetes. Autoantibody assays were repeated throughout the first 3 years of life to confirm the patient did not have an immune-mediated form of diabetes. In addition, antibody testing for additional autoimmunity, including celiac disease (anti-tissue transglutaminase 2 antibodies, antigliadin antibodies, both immunoglobulin G [IgG] and IgA) and autoimmune thyroiditis (anti-thyroperoxidase antibodies, anti-thyroid-stimulating hormone receptor antibodies), was consistently negative.

Since NDM is a rare condition that almost invariably recognizes a monogenic cause, with recessive forms more frequently found in consanguineous families (Barbetti et al., 2017), direct DNA sequencing of the most common PNDM genes (i.e., KCNJ11, INS, and ABCC8) was performed by the standard Sanger method, revealing a homozygous c.3G > A (p.Met1Ile; $INS^{ATG>ATA}$) mutation. This mutation is predicted to abrogate insulin translation initiation and cause a permanent form of NDM (Garin et al., 2010).

At the time of this study, the patient was 11 years old. He was reported to be overweight (height, 126.8 cm; weight, 41.5 kg; BMI, 25.8) and free from any diabetic-related complications. His treatment regimen consisted of insulin therapy at medium dose (0.66 UI/kg/day). His HbA1c level from age 3 to 11 was reported to range between 7.1% and 9.1% (54–76 mmol/mol).

$INS^{ATG>ATA}$ Mutation Can Be Corrected by CRISPR/Cas9 in Human Induced Pluripotent Stem Cells

We obtained a skin biopsy from the patient after parental informed consent and derived fibroblast cultures and reprogrammed the somatic skin cells to iPSCs using mRNA-mediated reprogramming. Two iPSC lines were derived, and one of the two was differentiation competent. This is consistent with the variable differentiation competence of iPSC lines (Sui et al., 2017). Stem cells contained the $INS^{ATG>ATA}$ mutation as determined by Sanger sequencing (Figure 1A). A guide RNA was designed against the INS locus close to the mutation site, along with a correction template with both the normal ATG and a neutral SNP. This neutral SNP prevented Cas9 activity on the corrected alleles and allowed us to distinguish the corrected allele from a wild-type allele (Figure 1C). Two days post transfection, Cas9-GFP-positive cells were sorted and clonally expanded. Genomic DNA was isolated to amplify and sequence the insulin ATG region. Sixty-one of 72 colonies were sequenced, with three showing the desired gene correction. Since the homozygous mutation originates from a consanguineous marriage, we were unable to test for heterozygosity in the vicinity of the insulin gene, which would have confirmed the correction of both alleles. Such testing can exclude the presence of a wild-type copy on one allele and a large deletion removing the primer-binding site on another allele (Egli et al., 2018). The possibility of introducing larger deletions has been addressed by others (Kosicki et al., 2018). Three top off-target sites were examined by PCR and Sanger sequencing. One cell line showed an off-target effect 1.7 kb upstream of the *PAX2* locus (Figure S1), a gene involved in nervous system development. To control for possible inadvertent changes to the genome through CRISPR/Cas9, three gene-corrected lines were utilized for *in vitro* experimentation in subsequent experiments. No differences were seen with regard to insulin expression. Last, to confirm the pluripotency of the gene-corrected stem cells, both mutant and corrected patient iPSCs were used for karyotyping and immune staining. All cell lines expressed pluripotent marker genes, OCT4 and SOX2, and had normal karyotypes (46/XY), including two copies of chromosome 11 (Figures 1B and 1D), where the *INS* gene resides, which excluded the possibility of chromosome loss or large chromosome abnormalities that might result in detection of only corrected alleles.

$INS^{ATG>ATA}$ Mutant Stem Cells Efficiently Differentiate to Insulin-Negative Endocrine Cells

To determine whether the mutant and the gene-corrected cells could differentiate to β-like cells, we used a stepwise differentiation protocol (Figure 2A) (Pagliuca et al., 2014; Rezania et al., 2014; Sui et al., 2017). There was no detectable difference in differentiation efficiency among mutant and corrected iPSCs. Both the insulin mutant and the corrected cells differentiated efficiently to the definitive endoderm (DE) stage, with 96% of cells positive for both SOX17 and FOXA2 (Figures 2B, S2A, and S2B). At the pancreatic progenitor (PP) stage, more than 40% of cells in both populations were double positive for PDX1 and NKX6.1 (Figures 2C, S2C, and S2D).

Upon further differentiation, *INS* mutant cells showed a lack of C-peptide-positive cells, while cells genetically corrected from mutated *INS* ATA to wild-type ATG showed 53.7% ± 9.8% insulin-positive cells (Figures 2D and 2E). To exclude the possibility that the loss of C-peptide-positive cells in mutant cells was due to differentiation failure, the quantification of the expression of markers of β cell differentiation, including *CHGA*, marking pancreatic endocrine cells, as well as *NKX6.1*, *PDX1*, and *MAFA*, marking pancreatic β cells, was conducted using immunostaining. These pancreatic endocrine and β cell

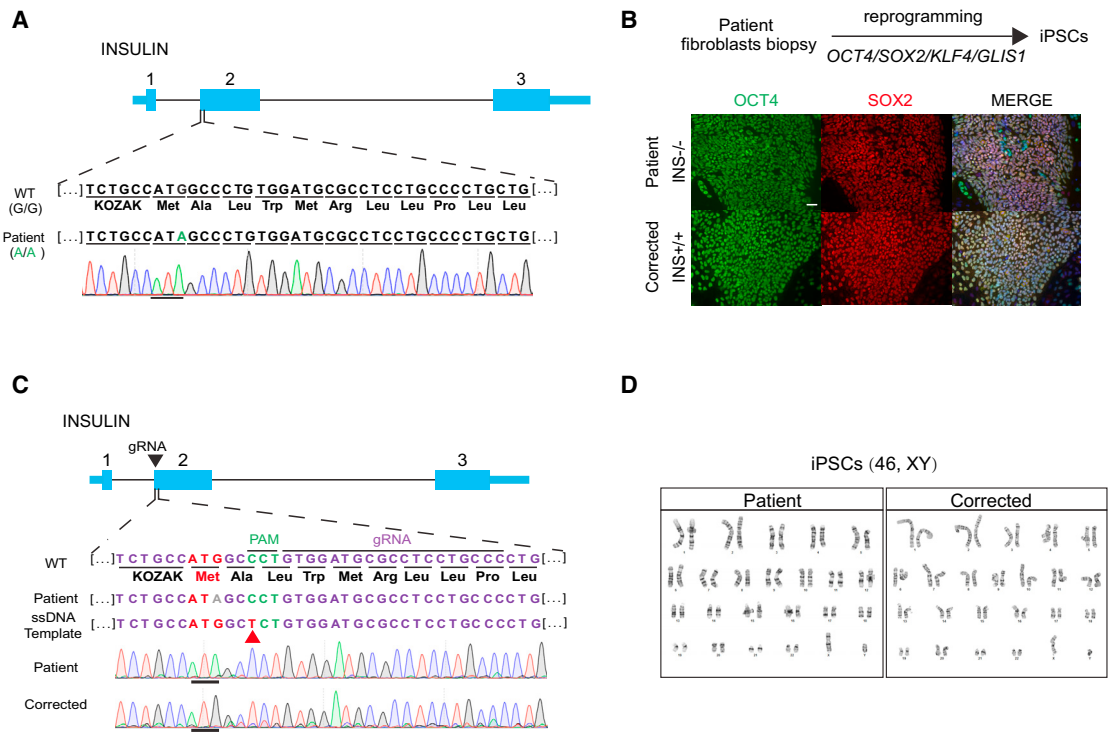

Figure 1. Genotyping at the Insulin Locus of a Patient with PNDM, and Gene Correction in Patient-Derived Stem Cells Using CRISPR/Cas9

(A) Sanger sequencing results at the start codon of the *INS* gene.

(B) Immunostaining for pluripotency genes OCT4 and SOX2 in mutant and corrected cells. Scale bar, 50 μm.

(C) Correction of $INS^{ATG>ATA}$ mutation in patient iPSCs by CRISPR/Cas9 using a single-stranded DNA (ssDNA) repair template. The neutral nucleotide polymorphism introduced is indicated by the red arrowhead. gRNA, guide RNA.

(D) Karyotypes of patient and gene-edited iPSCs (46/XY).

See also Figure S1.

markers were expressed in both mutant and corrected cells at comparable frequencies (Figure 2F–2I). Both mutant and corrected cell clusters contained 50%–60% pancreatic endocrine cells marked by expression of CHGA, with none of the cells with the $INS^{ATG>ATA}$ mutation showing insulin expression. Glucagon-positive cells were found at a frequency of 20.15% ± 3.2% and 21.2% ± 4.8% in mutant and corrected pancreatic clusters, respectively (Figure 2J). Therefore, most cells with *CHGA* expression did not express insulin, but expressed MAFA and NKX6.1, suggesting they are insulin-negative β-like cells. Approximately half the cells were NKX6.1 negative (Figures S2D and S2E), suggesting that not all insulin-positive cells showed the characteristics of stem cell-derived β (sc-β) cells.

Although insulin protein was not detected, quantitative RT-PCR for insulin mRNA confirmed the expression of the insulin locus. Expression levels of mutant insulin mRNA were reduced 800-fold compared with wild-type cells, possibly due to the reduced stability of a non-translated transcript (Figure 3A). Using gel electrophoresis after qRT-PCR, low levels of *INS* mRNA in the mutant cells were confirmed (Figure 3B), suggesting that the G > A mutation not only blocked *INS* translation but also affected mRNA stability. Interestingly, insulin-negative cells contained a lower amount of spliced *XBP1* than gene-corrected cells expressing insulin, suggesting that insulin production is directly responsible for the activation of the inositol-requiring enzyme 1α pathway of the unfolded protein response (Figures 3C and 3D).

To functionally characterize mutant and corrected stem cell-derived endocrine cells, we determined insulin content, pro-insulin content, and insulin secretion *in vitro* (Figures 3E–3G). Through an ultra-sensitive ELISA, we analyzed the insulin content, which we found to be restored from 0 pmol/cell in the mutant to 0.6 pmol/cell in corrected cells, comparable to wild-type human ESC-derived β-like cells (Figure 3E). Furthermore, no pro-insulin was detected in mutant β-like cells, while about 0.14 ± 0.03 pmol/L pro-insulin was detected after correction of the $INS^{ATG>ATA}$ mutation, which excludes the possibility that insulin loss was due

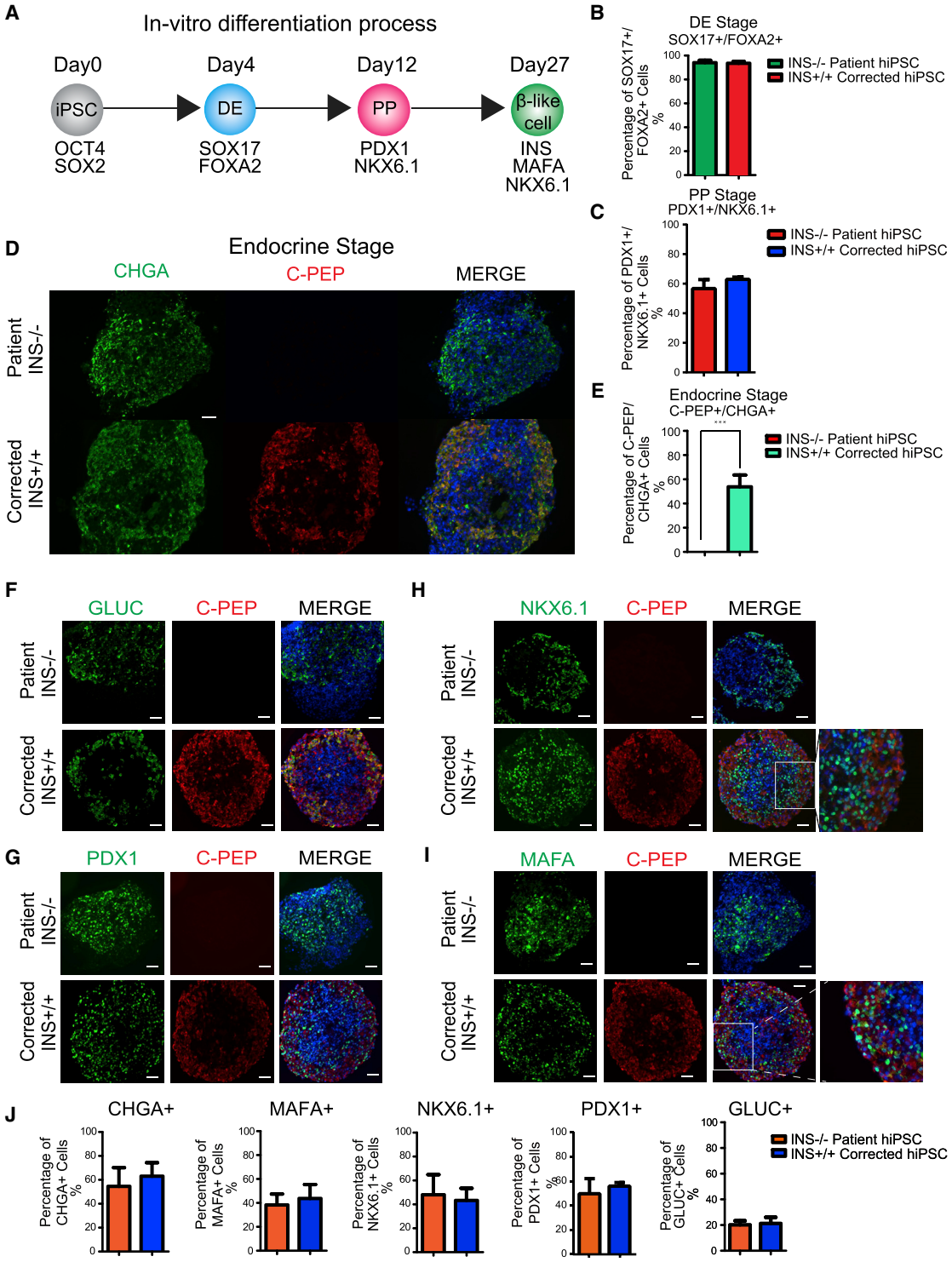

Figure 2. *INS*$^{ATG>ATA}$ Stem Cells Differentiate to Endocrine Cells without Insulin

(A) Schematic of *in vitro* β cell differentiation. Markers for specific stages of differentiation are indicated. DE, definitive endoderm; PP, pancreatic progenitors.

(B) Quantification results of cells immune-positive for both SOX17 and FOXA2 on day 4. n = 3 independent experiments. hiPSC, human iPSC.

(C) Quantification results of cells immune-positive for both PDX1 and NKX6.1 on day 12. n = 3 independent experiments.

(legend continued on next page)

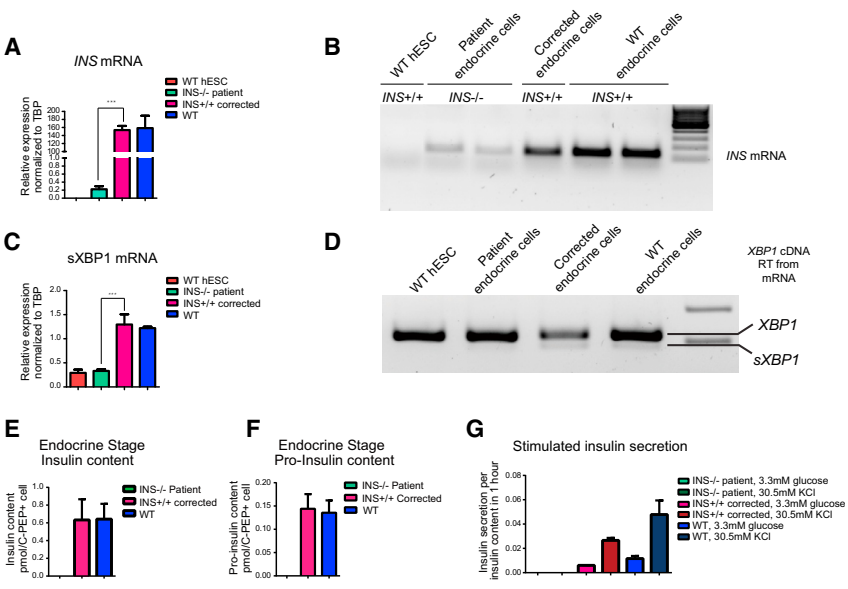

Figure 3. Gene Correction Restores Insulin Expression and Insulin mRNA Stability and Increases Spliced XBP-1

(A) *INS* mRNA quantitation results by qRT-PCR for *INS* mutant β-like cells in comparison with corrected and wild-type cells. n = 3 independent experiments. Data represent mean ± SD (***p < 0.001). hESC, human ESC; TBP, TATA-box binding protein; WT, wild-type.

(B) Agarose gel electrophoresis results for insulin mRNA after qRT-PCR.

(C) Spliced *XBP1* (*sXBP1*) mRNA quantitation results by qRT-PCR for *INS* mutant β-like cells in comparison with corrected and wild-type cells. n = 3 independent experiments. Data represent mean ± SD (***p < 0.001).

(D) RT-PCR results for *XBP1* and *sXBP1* mRNA using agarose gel electrophoresis.

(E) Analysis of insulin content using ELISA for *INS* mutant, corrected, and WT β-like cells. n = 3 independent experiments.

(F) Analysis of pro-insulin content using ELISA for *INS* mutant, corrected, and WT β-like cells. n = 3 independent experiments.

(G) Analysis of insulin secretion in *INS* mutant and corrected β-like cells using ELISA. Insulin secretion was analyzed under 3.3 mM glucose and 30.5 mM KCl conditions. n = 3 independent experiments. Significance was tested by Student's t test.

to the failure of pro-insulin processing in mutant cells (Figures 3F and S2F). To test insulin secretion in response to stimulation, the levels of secreted insulin in both mutant and corrected β cells subjected to KCl treatment were quantified. Whereas mutant cells failed to secrete any detectable levels of insulin, corrected cells secreted 0.006 ± 0.0002 pmol under basal conditions of 3.3 mM glucose and 0.027 ± 0.002 pmol insulin after stimulation by 30.5 mM KCl (Figure 3G). Glucose-stimulated insulin secretion was not evaluated *in vitro*, as these *in vitro* cells show only a modest increase, and are not equivalent to pancreatic β cells *in vivo* for several other parameters, including the ratio of pro-insulin to insulin (Sui et al., 2017). Taken together, we can conclude that insulin is not required for β cell differentiation, but mutant cells fail to produce insulin.

Gene-Corrected Endocrine Cells Maintain Normal Blood Glucose Homeostasis in Mice

To determine whether gene correction resulted in functional endocrine cells, stem cell-derived clusters were grafted into the leg muscle of immune-compromised mice (Figure 4A). Both mutant cells and gene-corrected cells were grafted into a total of eight mice (four for mutant and four for corrected cells). We analyzed the amount of human C-peptide in transplanted mouse blood at 2-week intervals over the course of 6 months in daytime measurements of *ad lib* fed mice on standard diet. None of the four mice grafted with mutant cells showed detectable serum C-peptide. In mice grafted with corrected cells, human C-peptide became detectable starting from 3 weeks in two of the four mice (Figure 4B). One mouse from the group grafted with corrected cells was lost after 7 weeks post transplantation due to unknown cause. Of the remaining three mice, two were C-peptide positive, with C-peptide levels gradually increasing until 19 weeks post transplantation (Figure 4B). To determine whether corrected cells were able to adapt insulin secretion to changes in blood glucose, we fasted mice and analyzed human insulin levels before and after re-feeding at 11 weeks post transplantation. We were able to see a decrease in human C-peptide during

(D) Immunostaining results for C-peptide (C-PEP) and chromogranin (CHGA) on day 27 after differentiation. Scale bar, 50 μm.

(E) Quantification results of cells immune-positive for both C-peptide and CHGA on day 27 after differentiation. n = 3 independent experiments. Data represent mean ± SD (***p < 0.001).

(F–I) Immunostaining results for glucagon (GLUC) (F), PDX1 (G), NKX6.1 (H), and MAFA (I), co-stained with C-peptide in *INS* mutant and corrected cells. Scale bar, 50 μm.

(J) Quantification results of cells immune-positive for CHGA, MAFA, NKX6.1, PDX1, and GLUC in *INS* mutant and corrected cells. n = 3 independent experiments. Significance was tested by Student's t test.

See also Figure S2.

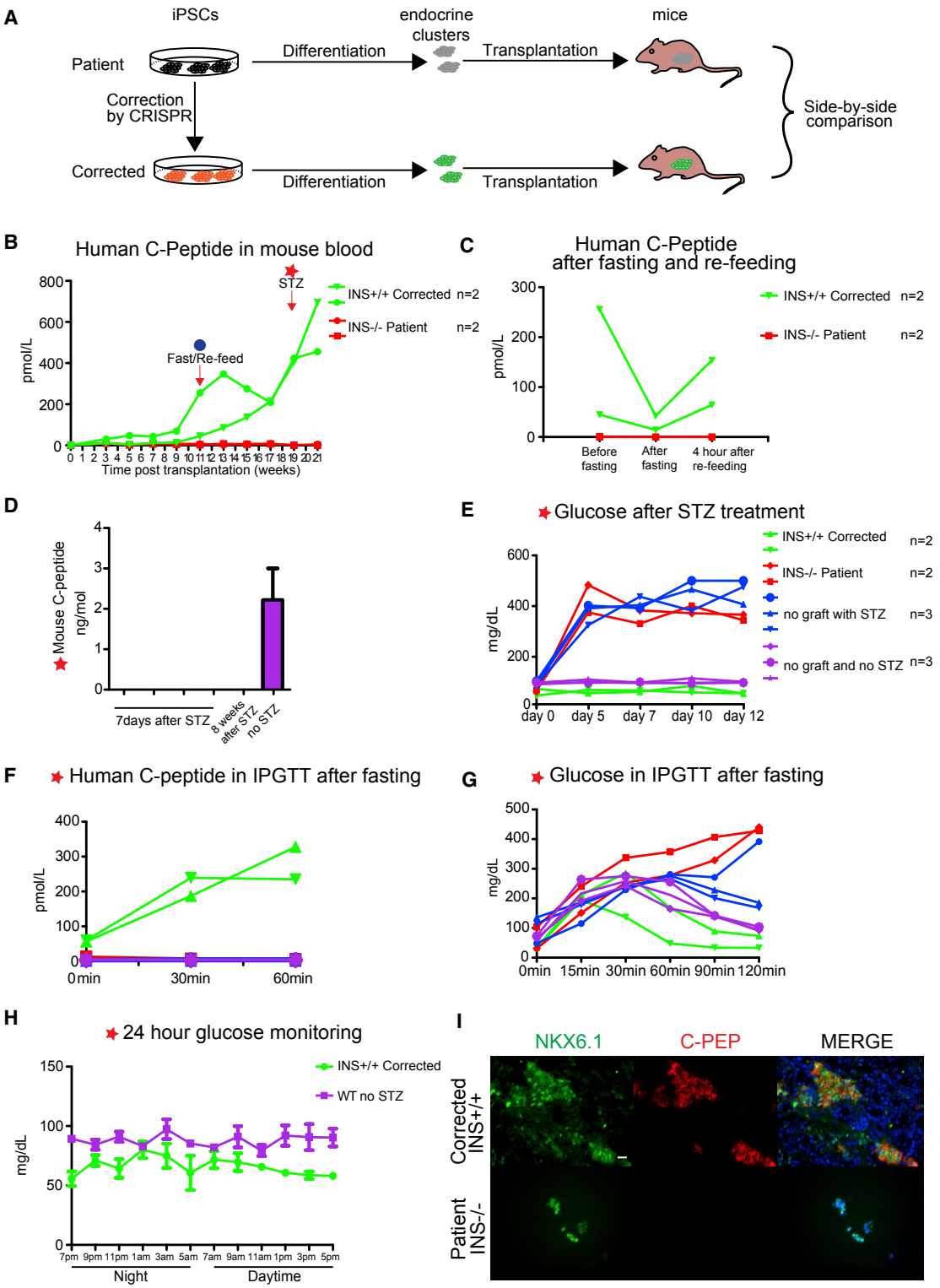

Figure 4. *In Vivo* Functional Analysis of Endocrine Cells Derived from *INS* Mutant and Corrected Patient iPSCs

(A) Schematics of *in vitro* and *in vivo* functional assays for side-by-side comparison of *INS* mutant and corrected endocrine cells.

(B and C) *In vivo* functional analysis of endocrine cells. (B) Human C-peptide in mouse blood after transplantation. STZ treatment was induced once C-peptide levels reached >400 pM or after 19 weeks of transplantation. (C) Human C-peptide in mouse blood after fasting and re-feeding at 11 weeks.

(legend continued on next page)

fasting, followed by a substantial increase post re-feeding (Figure 4C).

Last, to determine whether corrected β-like cells were able to protect mice from diabetes, we treated mice with 150 mg/kg STZ after human C-peptide reached a threshold of >400 pM or at 19 weeks post transplantation (Figure 4B). By measuring levels of C-peptide, we were able to confirm that STZ treatment had effectively eliminated insulin secretion from mouse β cells (Figure 4D). Both mice grafted with mutant cells and non-grafted mice (n = 3) became diabetic 7 days post STZ treatment (Figure 4E). In contrast, mice grafted with corrected human cells maintained normal blood glucose levels (Figure 4E). These mice had continuous access to food.

Upon fasting and intraperitoneal injection of glucose (intraperitoneal glucose tolerance test), human C-peptide increased in the serum (Figure 4F), and blood glucose levels normalized in mice grafted with gene-corrected cells, but not with mutant ones (Figure 4G). One mouse was kept for more than 8 weeks after STZ treatment, and tested during a 24 hr time course for glucose homeostasis. As mouse C-peptide remained undetectable at 8 weeks after STZ treatment (Figure 4D), glucose regulation was due to the graft, rather than attributable to mouse β cell regeneration after STZ treatment. Prior studies have shown that blood glucose levels vary by circadian rhythm, with daytime measures showing a trend toward normoglycemia, and nighttime measures showing hyperglycemia (King et al., 2017). We found that in mice with continuous access to food, glucose levels averaged 64 mg/dL, and did not exceed 100 mg/dL regardless of the time of day (Figure 4H). Therefore, the graft normalized blood glucose levels throughout the day.

To determine whether the graft contained endocrine cells, grafted human tissue was removed and stained for both NKX6.1 and insulin. NKX6.1-positive cells were found in both mutant and corrected cell grafts (Figure 4I). Only gene-corrected cells showed insulin expression in islet-like clusters, while non-corrected cells showed Nkx6.1-positive insulin-negative cells (Figure 4I). Importantly, insulin-positive cells were also positive for Nkx6.1, indicative of mature sc-β cells (Pagliuca et al., 2014; Rezania et al., 2014). However, six of the eight grafted mice formed large growths within 20 weeks of transplantation and had to be sacrificed thereafter. The grafts also contained cell types other than endocrine cells, as shown by H&E staining (Figure S3).

DISCUSSION

Here we report a proof-of principle study for the use of cell replacement therapy as a treatment for diabetes caused by a single gene mutation. After the identification in a patient with PNDM of a homozygous ATG > ATA mutation at codon 1 of the insulin gene, leading to the deletion of methionine 1, the mutation was reverted to wild-type ATG using CRISPR/Cas9, and both mutant and corrected cells were differentiated to pancreatic endocrine cells. Although insulin is the defining protein of a β cell, we found that it was dispensable for differentiation, as we were able to obtain insulin-negative cells expressing key β cell markers, including PDX1, MAFA, and NKX6.1. Such insulin-negative β-like cells may be useful in future studies for investigating the role of insulin in endoplasmic reticulum stress-mediated β cell failure, and for the investigation of insulin epitopes in autoimmune diabetes.

Transplanted endocrine cells derived from the corrected patient stem cells were shown to produce detectable levels of insulin that allowed for the sustenance of normoglycemia in the respective mouse models. It should be noted, however, that in six of eight grafted mice, teratomas formed within 20 weeks post transplantation. We also noted that the iPSCs from the patient with or without correction generally resulted in small cell clusters because of cell death during differentiation. This points to persistent inefficiencies and variability in the differentiation of iPSCs to different lineages (Nishizawa et al., 2016; Sui et al., 2017). Furthermore, the CRISPR tools used here confirm the occurrence of off-target effects. Despite these challenges, our data show that endocrine cells from patients with monogenic forms of diabetes can potentially be used for cell replacement upon gene correction, if teratoma formation and off-target effects can reliably be avoided.

For patients with mutations in the insulin locus (Colombo et al., 2008; Stoy et al., 2007), as well as other forms of monogenetic diabetes, a cell therapy using autologous cells may not require immune protection. Short of grafting

(D) Mouse C-peptide 7 days and 8 weeks after STZ treatment. n = 4 independent experiments.
(E) Mouse blood glucose levels after STZ treatment, daytime measurements. n = 2 mice transplanted with $INS^{+/+}$-corrected or $INS^{-/-}$ patient endocrine cells; n = 3 mice without transplantation or without both transplantation and STZ treatment.
(F and G) Intraperitoneal glucose tolerance test (IPGTT) results after STZ treatment in mutant and corrected cells-transplanted mice.
(F) Human C-peptide ELISA results during IPGTT. (G) Mouse blood glucose measurement results during IPGTT.
(H) Results for 24 hr glucose monitoring. n = 3 independent experiments.
(I) Immunostaining for insulin and Nkx6.1 of *in vivo* graft tissue from transplanted mice. Scale bar, 20 μm.
See also Figure S3.

them into a patient, tolerance to autologous cells may be studied in mice with an autologous immune system (Kalscheuer et al., 2012), but ultimately, conclusive answers to these questions will only be learned by grafting cells into patients. In contrast to diabetes caused by single-gene mutations, T1D likely requires two key interventions, cell therapy as well as immune protection, each associated with its own challenges. Diabetes caused by single-gene mutations are not rare, accounting for an estimated 1%–5% of all diabetes cases (Fajans and Bell, 2011; Shields et al., 2010), and are particularly common in pediatric diabetes (Delvecchio et al., 2017). Therefore, monogenic diabetes may provide a suitable initial clinical target for autologous stem cell-based therapies for diabetes.

EXPERIMENTAL PROCEDURES

All experiments with human cells were reviewed and approved by the Columbia Institutional Review Board. Human fibroblasts were obtained after informed consent of the legal guardians of the patient at Salesi Hospital. Genetic analysis was done with IRB approval at University of Rome Tor Vergata where FB is Associate Professor of Clinical Biochemistry and Molecular Biology. Animal experiments were performed according to a protocol approved by the Columbia University Institutional Animal Care and Use Committee. Animal assignments to the treatment and control groups were not blinded.

In Vitro Differentiation and Analysis Methods

For *in vitro* pancreatic endocrine cell differentiation, we used a previously described protocol (Sui et al., 2017). Briefly, mutant and corrected human iPSCs routinely cultured in KOSR-based human ESC culture medium to 90% confluence were passaged with TrypLE (12605036, Life Technologies) and 1 million dissociated cells were seeded onto Matrigel-coated plates in mTeSR1 medium (05,850, STEMCELL Technologies) containing 5 μM Y26732. After 24 hr, β cell differentiation was started by replacing mTeSR1 medium with STEMDiff Endoderm Differentiation Kit (05,110, STEMCELL Technologies). DE differentiation took 4 days followed by PP differentiation. After 8 days, DE cells progressed to the PP stage by treatment with fibroblast growth factor 7-containing medium for 2 days, All-*trans*-retinoic acid (04-0021, Stemgent)- and LDN193189 (04-0074, Stemgent)-containing medium for 3 days, and epidermal growth factor (236-EG, R&D Systems)-containing medium for another 3 days. Upon reaching the PP stage, cells were dissociated into single cells, aggregated to clusters (4×10^4 cells per cluster), and cultured on low-attachment 96-well plates (7007, Corning) for 2 more weeks with medium containing mainly activin receptor-like kinase 5 inhibitor (04-0015, Stemgent) and zinc sulfate (Z0251-100G, Sigma-Aldrich). In addition to patient mutant and corrected iPSCs, the human ESCs Mel1 that contained a knockin of GFP in the insulin locus and a wild-type allele were used in this study as a control for some experiments (Micallef et al., 2012). Wild-type control cells therefore contain one functional insulin allele.

At day 27, five clusters were fixed with 4% paraformaldehyde (PFA) solution in PBS (sc-281692, Santa Cruz Biotechnology) for immune staining. We used 30 clusters to assay insulin content and insulin secretion for analysis by Mercodia Insulin ELISA (10-1113-01, Mercodia, 1 μIU/mL = 6 pmol/L). Sixty clusters were used for RNA extraction. The detailed differentiation protocol, including medium formulations and chemical/growth factor components information is provided in Tables S3 and S4.

Immunostaining and Image Processing Procedure

For cluster/tissue immune staining, clusters were first fixed with 4% PFA for 1 hr and incubated with 30% sucrose overnight. After sucrose treatment, clusters were embedded in Tissue-Tek O.C.T. Compound (4583, Amazon), snap-frozen on dry ice, and kept at −80°C before sectioning. Afterward, O.C.T. embedded clusters were sectioned, and sectioned slides were blocked with donkey serum (D9663-10ML, Sigma-Aldrich) and permeabilized with 0.1% Triton (9002-93-1, Sigma-Aldrich) in PBS. Following blocking and permeabilization, cluster sections on the slides were incubated with primary antibody overnight at 4°C and stained with secondary antibody for 1 hr at room temperature. After counterstaining with DAPI (D3571, Thermo Fisher Scientific), slides were used for taking pictures under a fluorescence microscope (Olympus IX73). For each differentiation experiment, we randomly picked five clusters for sectioning and staining. On average, 15 pictures per primary antibody were taken for the five randomly picked clusters and processed by ImageJ with the same parameters to calculate percentage of cells staining positive. First, the DAPI channel was used to pre-determine average total cell number from those 15 pictures after channel splitting. Next, single- or double-positive cell numbers for the primary antibodies were calculated from other channels and averaged for the 15 pictures. Finally, the percentage of single- or double-positive cells was obtained by dividing the average total cell number by the average single- or double-positive cell number. The investigator was not blinded in this analysis. Information on primary and secondary antibodies used in the study is provided in Table S2.

For H&E staining for grafted tissues, a previously published protocol was followed (Fischer et al., 2008).

Statistical Analysis

Student's t tests for detecting significance of biological difference were used for all statistical measures. All experiments in the paper were conducted with at least three independent experiments unless otherwise stated. "n" in the paper indicates the independent experimental number.

SUPPLEMENTAL INFORMATION

Supplemental Information includes Supplemental Experimental Procedures, three figures, and four tables and can be found with this article online at https://doi.org/10.1016/j.stemcr.2018.11.006.

AUTHOR CONTRIBUTIONS

S.M. and D.E. conceived the project and designed experiments. S.M. performed all experiments and analyzed the data. R.V.

generated iPSCs from patient skin fibroblast cells and performed Cas9 off-target effect analysis. L.S. assisted with stem cell differentiation and transplantation experiments. V.C. and F.B. diagnosed the patient, derived the skin biopsy, identified the mutation, and provided clinical data. S.M. and D.E. wrote the paper.

ACKNOWLEDGMENTS

This work was supported by the American Diabetes Association (grant #1-16-ICTS-029) and the Italian Ministry of Health (project PE-2011-02350284). S.M. is the recipient of a Chinese scholarship from the China Scholarship Council. D.E. is an NYSCF-Robertson investigator. We thank Danielle Baum for critical reading of the manuscript.

Received: November 30, 2017
Revised: November 2, 2018
Accepted: November 5, 2018
Published: November 29, 2018

REFERENCES

Agulnick, A.D., Ambruzs, D.M., Moorman, M.A., Bhoumik, A., Cesario, R.M., Payne, J.K., Kelly, J.R., Haakmeester, C., Srijemac, R., Wilson, A.Z., et al. (2015). Insulin-producing endocrine cells differentiated in vitro from human embryonic stem cells function in macroencapsulation devices in vivo. Stem Cells Transl. Med. *4*, 1214–1222.

Barbetti, F., Mammì, C., Liu, M., Grasso, V., Arvan, P., Remedi, M., and Nichols, C. (2017). Neonatal diabetes: permanent neonatal diabetes and transient neonatal diabetes. Front. Diabetes *25*, 1–25.

Bonner-Weir, S., and Orci, L. (1982). New perspectives on the microvasculature of the islets of Langerhans in the rat. Diabetes *31*, 883–889.

Colombo, C., Porzio, O., Liu, M., Massa, O., Vasta, M., Salardi, S., Beccaria, L., Monciotti, C., Toni, S., Pedersen, O., et al. (2008). Seven mutations in the human insulin gene linked to permanent neonatal/infancy-onset diabetes mellitus. J. Clin. Invest. *118*, 2148–2156.

Delvecchio, M., Mozzillo, E., Salzano, G., Iafusco, D., Frontino, G., Patera, P.I., Rabbone, I., Cherubini, V., Grasso, V., Tinto, N., et al. (2017). Monogenic diabetes accounts for 6.3% of cases referred to 15 Italian pediatric diabetes centers during 2007 to 2012. J. Clin. Endocrinol. Metab. *102*, 1826–1834.

Egli, D., Zuccaro, M., Kosicki, M., Church, G., Bradley, A., and Jasin, M. (2018). Inter-homologue repair in fertilized human eggs? Nature *560*, E5–E7.

Fajans, S.S., and Bell, G.I. (2011). MODY: history, genetics, pathophysiology, and clinical decision making. Diabetes Care *34*, 1878–1884.

Fischer, A.H., Jacobson, K.A., Rose, J., and Zeller, R. (2008). Hematoxylin and eosin staining of tissue and cell sections. CSH Protoc. https://doi.org/10.1101/pdb.prot4986.

Garin, I., Edghill, E.L., Akerman, I., Rubio-Cabezas, O., Rica, I., Locke, J.M., Maestro, M.A., Alshaikh, A., Bundak, R., del Castillo, G., et al. (2010). Recessive mutations in the INS gene result in neonatal diabetes through reduced insulin biosynthesis. Proc. Natl. Acad. Sci. U S A *107*, 3105–3110.

Kalscheuer, H., Danzl, N., Onoe, T., Faust, T., Winchester, R., Goland, R., Greenberg, E., Spitzer, T.R., Savage, D.G., Tahara, H., et al. (2012). A model for personalized in vivo analysis of human immune responsiveness. Sci. Transl. Med. *4*, 125ra130.

King, A.J., Austin, A.L., Nandi, M., and Bowe, J.E. (2017). Diabetes in rats is cured by islet transplantation...but only during daytime. Cell Transplant. *26*, 171–172.

Kosicki, M., Tomberg, K., and Bradley, A. (2018). Repair of double-strand breaks induced by CRISPR-Cas9 leads to large deletions and complex rearrangements. Nat. Biotechnol. *36*, 765–771.

Micallef, S.J., Li, X., Schiesser, J.V., Hirst, C.E., Yu, Q.C., Lim, S.M., Nostro, M.C., Elliott, D.A., Sarangi, F., Harrison, L.C., et al. (2012). INS(GFP/w) human embryonic stem cells facilitate isolation of in vitro derived insulin-producing cells. Diabetologia *55*, 694–706.

Nishizawa, M., Chonabayashi, K., Nomura, M., Tanaka, A., Nakamura, M., Inagaki, A., Nishikawa, M., Takei, I., Oishi, A., Tanabe, K., et al. (2016). Epigenetic variation between human induced pluripotent stem cell lines is an indicator of differentiation capacity. Cell Stem Cell *19*, 341–354.

Pagliuca, F.W., Millman, J.R., Gurtler, M., Segel, M., Van Dervort, A., Ryu, J.H., Peterson, Q.P., Greiner, D., and Melton, D.A. (2014). Generation of functional human pancreatic beta cells in vitro. Cell *159*, 428–439.

Rezania, A., Bruin, J.E., Arora, P., Rubin, A., Batushansky, I., Asadi, A., O'Dwyer, S., Quiskamp, N., Mojibian, M., Albrecht, T., et al. (2014). Reversal of diabetes with insulin-producing cells derived in vitro from human pluripotent stem cells. Nat. Biotechnol. *32*, 1121–1133.

Sato, Y., Endo, H., Okuyama, H., Takeda, T., Iwahashi, H., Imagawa, A., Yamagata, K., Shimomura, I., and Inoue, M. (2011). Cellular hypoxia of pancreatic beta-cells due to high levels of oxygen consumption for insulin secretion in vitro. J. Biol. Chem. *286*, 12524–12532.

Shields, B.M., Hicks, S., Shepherd, M.H., Colclough, K., Hattersley, A.T., and Ellard, S. (2010). Maturity-onset diabetes of the young (MODY): how many cases are we missing? Diabetologia *53*, 2504–2508.

Stoy, J., Edghill, E.L., Flanagan, S.E., Ye, H., Paz, V.P., Pluzhnikov, A., Below, J.E., Hayes, M.G., Cox, N.J., Lipkind, G.M., et al. (2007). Insulin gene mutations as a cause of permanent neonatal diabetes. Proc. Natl. Acad. Sci. U S A *104*, 15040–15044.

Sui, L., Danzl, N., Campbell, S.R., Viola, R., Williams, D., Xing, Y., Wang, Y., Phillips, N., Poffenberger, G., Johannesson, B., et al. (2017). Beta cell replacement in mice using human type 1 diabetes nuclear transfer embryonic stem cells. Diabetes *67*, 26–35.

Vegas, A.J., Veiseh, O., Gurtler, M., Millman, J.R., Pagliuca, F.W., Bader, A.R., Doloff, J.C., Li, J., Chen, M., Olejnik, K., et al. (2016). Long-term glycemic control using polymer-encapsulated human stem cell-derived beta cells in immune-competent mice. Nat. Med. *22*, 306–311.

Stem Cell Reports, Volume *11*

Supplemental Information

β Cell Replacement after Gene Editing of a Neonatal Diabetes-Causing Mutation at the Insulin Locus

Shuangyu Ma, Ryan Viola, Lina Sui, Valentino Cherubini, Fabrizio Barbetti, and Dieter Egli

Figure S1. Related to Figure 1.

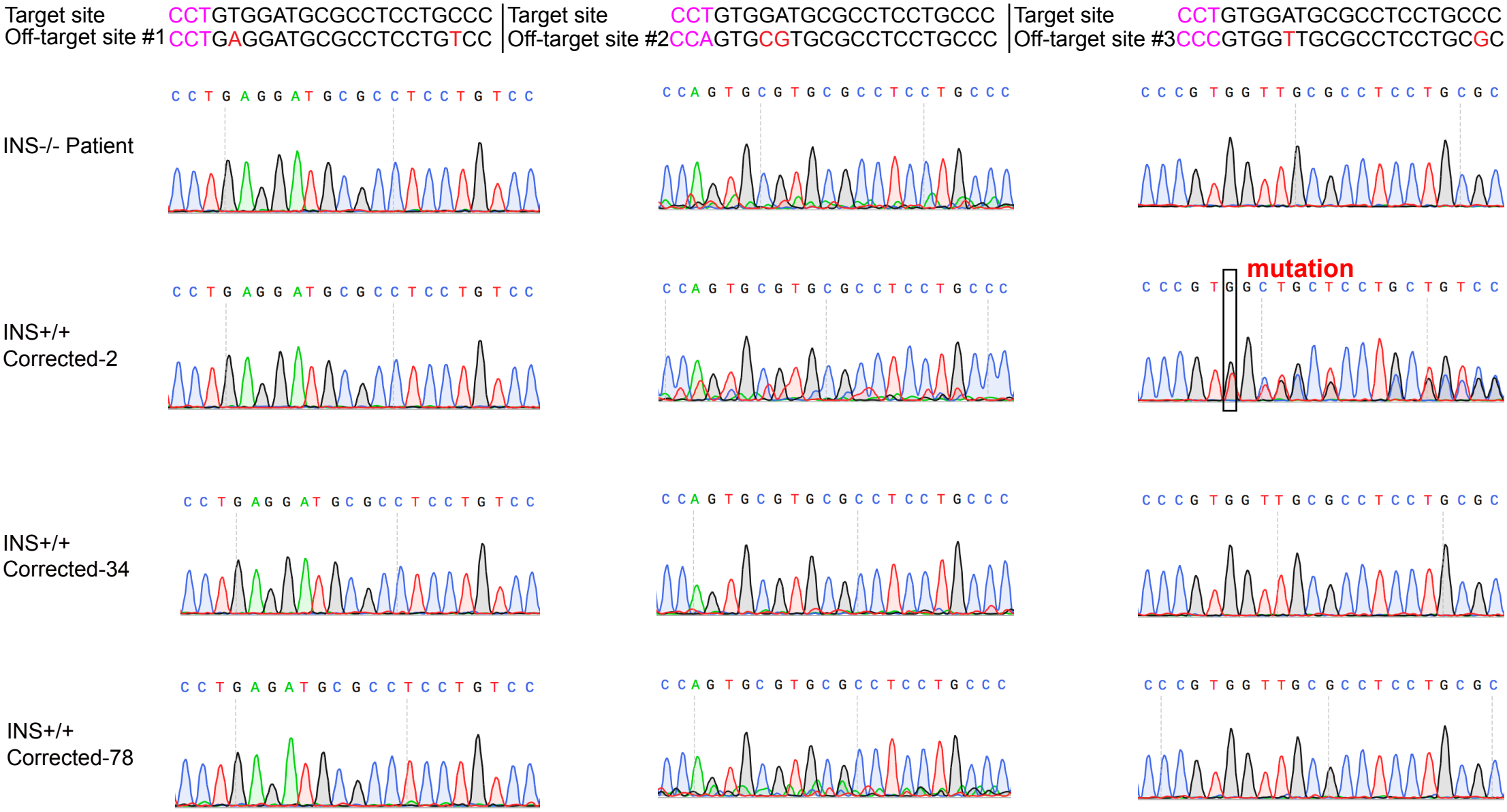

Figure S1. Off-target effect analysis at three top sites using PCR and Sanger sequencing, Related to Figure 1.

The top three off-target sites where chosen based on results (http://crispr.mit.edu/). Mismatches are highlighted in red. The site with an off-target effect is in a noncoding region 1.7kb upstream of the *PAX2* locus, a gene that is not expressed at detectable levels in stem cell derived endocrine cells.

Figure S2. Related to Figure 2.

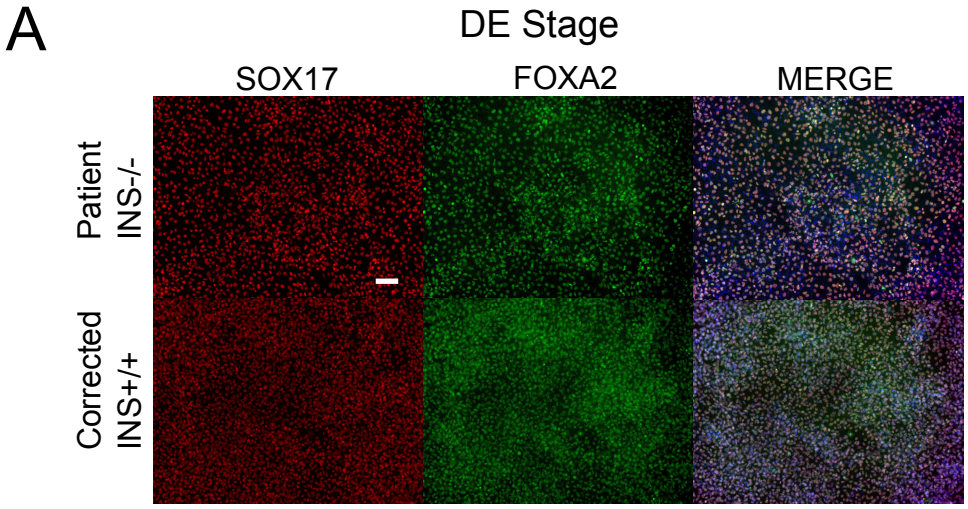

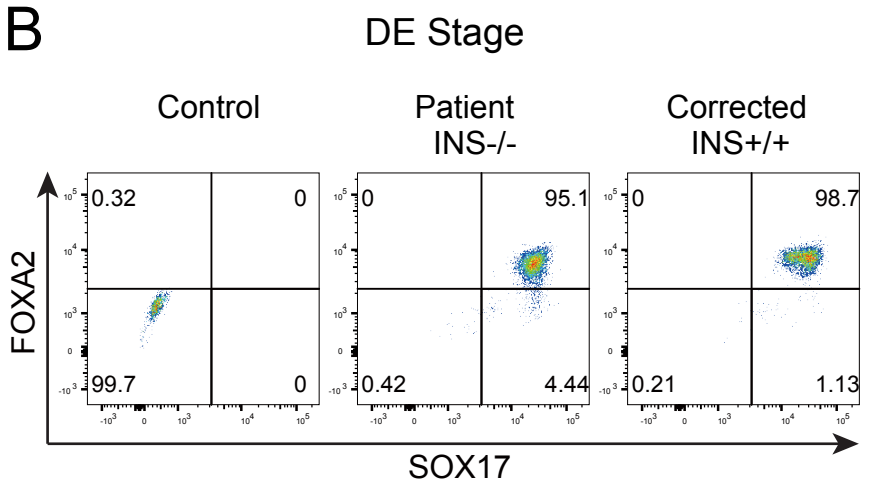

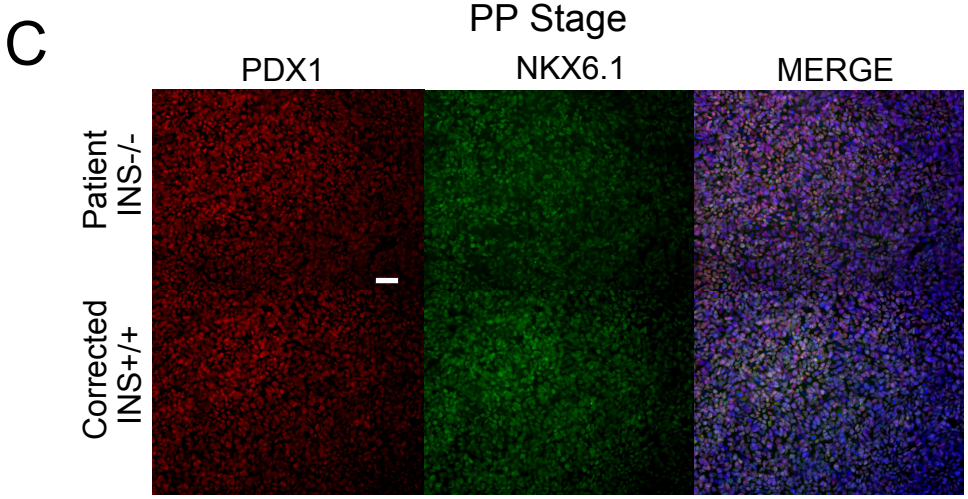

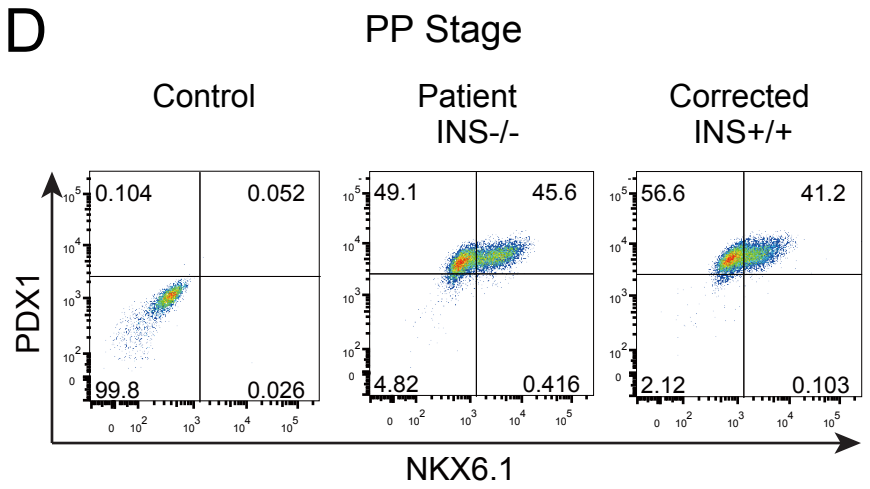

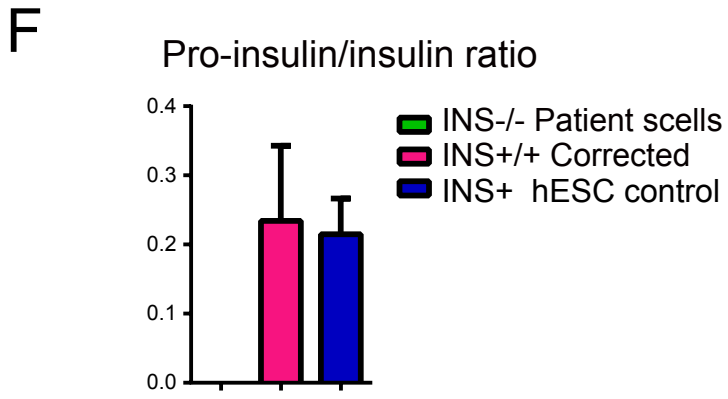

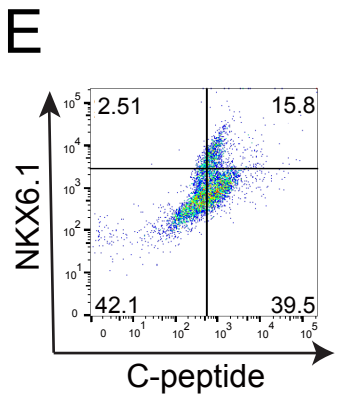

Figure S2. DE and PP differentiation results for mutant and corrected patient iPSCs, Related to Figure 2.

(A) Immuno-staining for DE marker genes, *SOX17* and *FOXA2*. Scale bar is 100 μM. (B) Flow cytometry results for DE marker genes, *SOX17* and *FOXA2.* (C) Immuno-staining for PP marker genes, *NKX6.1* and *PDX1*. Scale bar is 50 μM. (D) Flow cytometry results for PP marker genes, *NKX6.1* and *PDX1*. (E) Flow cytometry for Nkx6.1 and insulin. (F) Pro-insulin to insulin ratio results for *INS* mutant, corrected and WT β-like cells. n = 3 independent experiments.

Figure S3. Related to Figure 4.

INS-/- graft tissue

INS+/+ graft tissue

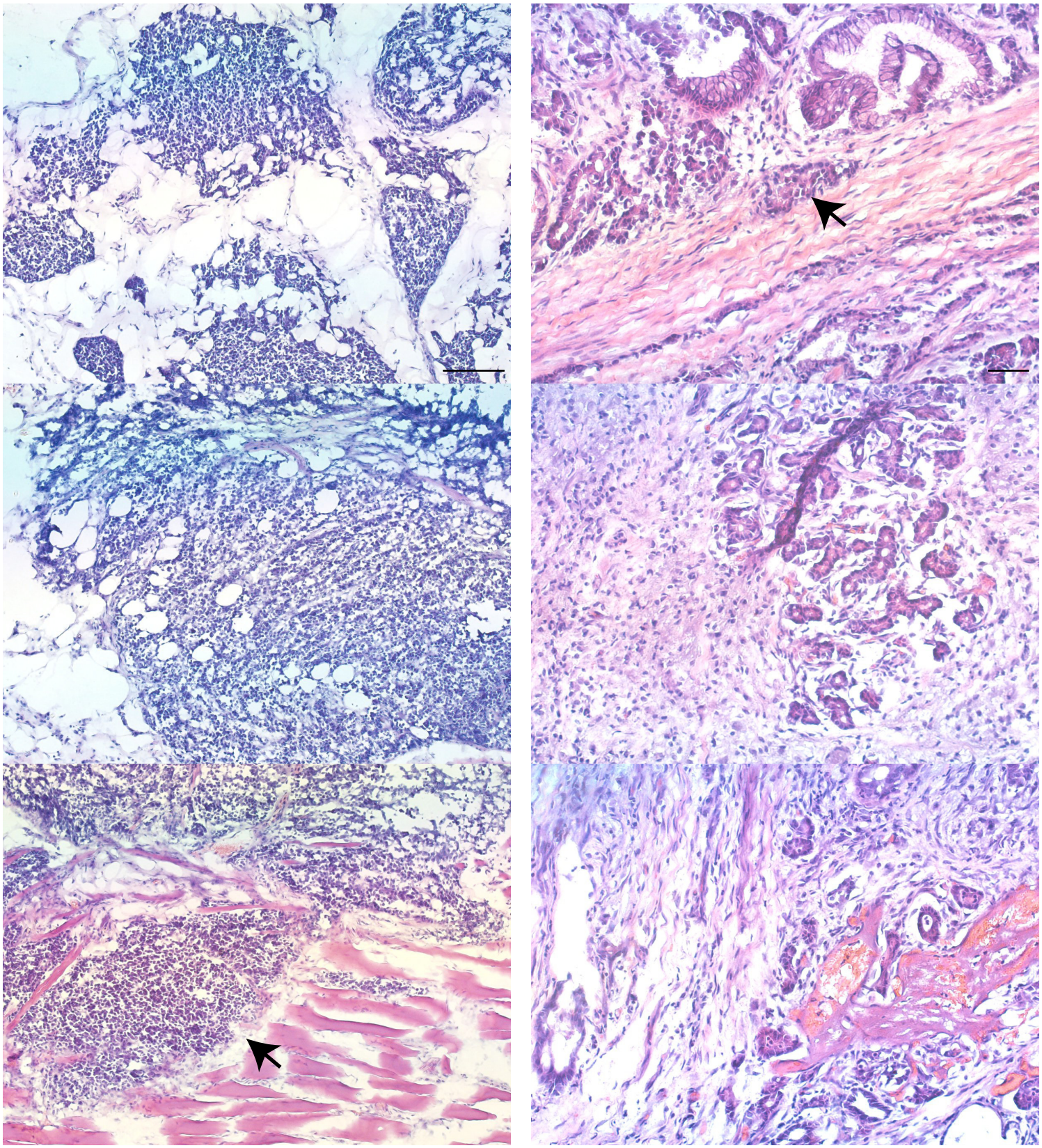

Figure S3. H&E staining of grafts, Related to Figure 4. Arrow points to a cluster of endocrine cells. Growth of non-pancreatic cells is also seen. Scale bar for INS+/+ is 50 μm and for INS-/- is 5 mm.

Supplemental Table 1. Primer, gRNA and ssODN sequences used in this study, Related to Figure 1 and 3.

Primer sequences used in this study:

gene	Primers
PTV3.6 (for PCR)	CATCAAGCAGGTCTGTTCCA
	CGGGTCTTGGGTGTGTAGAA
span PTV3.6 (for sequence)	GTCAGGTGGGCTCAGGATT
Insulin (for qPCR)	TTCTACACACCCAAGACCCG
	CAATGCCACGCTTCTGC
TBP (for qPCR)	AACAACAGCCTGCCACCTTA
	GCCATAAGGCATCATTGGAC
XBP1 and sXBP1 (for gel imaging)	GAAGCCAAGGGGAATGAAGT
	GGGAAGGGCATTTGAAGAAC
Spliced-XBP1 (for qPCR)	CTGAGTCCGCAGCAGGTG
	TGCCCAACAGGATATCAGACT
Off-target #1	CAAGTGACCCTCCTGAAACG
	AGCCAGTTTCCAGAATGACC
Off-target #2	TCTCTGTGAAGCCTGTGTGG
	CCAGAAAGACGTCCACTTCC
Off-target #3	GGATTCGGGCTGCAAGAG

gRNA and ssODN sequences used in this study:

gRNA Sequence(5' →3')	**ssDNA Sequence**	**Location**
CCTGTGGATGCGCCTCCTGC CC	tgagcccaggggccccaaggcagggcacctggccttcagcct gcctcagccctgcctgtctcccagATCACTGTCCTTC TGCCATGGCtCTGTGGATGCGCCTCCTGC CCCTGCTGGCGCTGCTGGCCCTCTGGGG ACCTGACCCAGCCGCAGCCTTTGTGAA CCAACACCTGTGCGGCTCACACCTGGT GGAAGCTCT	*INS* exon2

Red highlights indicates PAM sequence and Yellow highlights indicates *INS* mutation site.

Supplemental Table 2. Primary and Secondary Antibody dilution used in this study, Related to Figure 1 and 2.

Primary Antibody	**Dilution**
Anti-Rabbit FOXA2	1:400
Anti-Goat SOX17	1:100
Anti-Mouse NKX6.1	1:300
Anti-Goat PDX1	1:100
Anti-Mouse CHGA	1:100
Anti-Rabbit MAFA	1:100
Anti-Rat C-peptide	1:100
Anti-Guinea Pig Glucagon	1:200
Anti-Mouse OCT4	1:200
Anti-Rabbit SOX2	1:200
Secondary Antibody	**Dilution**
Donkey Anti-Rat Alexa Fluor® 488	1:500
Goat Anti-Rat Alexa Fluor® 555	1:500
Donkey Anti-Rabbit Alexa Fluor® 555	1:500
Donkey Anti-Rabbit Alexa Fluor®488	1:500
Donkey Anti-Guinea Pig Alexa Fluor®647	1:500
Donkey Anti-Goat Alexa Fluor® 555	1:500
Donkey Anti-Goat Alexa Fluor® 488	1:500
Donkey Anti-Mouse Alexa Fluor® 488	1:500
Donkey Anti-Mouse Alexa Fluor® 555	1:500
Goat anti-Rabbit IgG (H+L), HRP	1:500

Supplemental Table 3. Stem cell differentiation protocol, Related to Figure 2.

Stage	Day	Basal Media	Supplement
S0(1d)	d0	seeded 1×10^6 hiPSCs on matrigel (1×100) coated plates with 5μM Y-27632 in mTeSR1 for 24 hours	
S1(1d)	d1	M1 start differentiation until cells are 100% confluent and monolayer	Supplement A 1×100 Supplement B 1×100
S2(3d)	d2-4 change medium every 36 hours	M1 at the end of d4, check DE stage markers	Supplement B 1×100
S3(2d)	d5-6 no changing	M2	FGF7 50ng/ml
S4(3d)	d7-9 change medium every 36 hours	M3	KAAD 0.25μM RA 2μM LDN 250nM
S5(3d)	d10-12 change medium every 36 hours	M3 at the end of d12, check PP stage markers	EGF 50ng/ml
S6(2d)	d13-14 no need to change medium and don't move plates	M3 use Tryple-LE gently dissociate cells into single cells, aggregate 4×10^4 cells per cluster into low attachment 96 well plates	KAAD 0.25μM T3 1μM Alk5i 10μM Zinc-Sulfate 10μM Heparin 10μg/ml Y-27632 5μM
S7(7d)	d15-21 change medium every 2 days	M3	LDN 100nM T3 1μM Alk5i 10μM Zinc Sulfate 10μM DBZ 10μg/ml Heparin 10μg/ml
S8(7d)	d22-28 change medium every 2 days	M3 transfer every 48 clusters into 1 well of low attachment 6 well plates	T3 1μM Alk5i 10μM Zinc-Sulfate 10μM Heparin 10μg/ml N-Cys 1mM Trolox 10μM R428 2μM

Supplemental Table 4. Basal medium, chemical and other components for stem cell differentiation protocol, Related to Figure 2.

Basal medium for stem cell differentiation protocol:

Basal Medium name	Component
M1	Stemdiff™ Definitive Endoderm Basal Medium
M2	RPMI-1640 Penstrep 1×100 B-27 Serum free Supplement (50×)
M3	DMEM with high glucose, GlutamaxtTM Supplement, pyruvate Penstrep 1×100 B-27 Serum free Supplement (50×)

Chemicals and other components used in this study:

Component	Vendor	Cat. No.
DMEM with high glucose	Thermo fisher Scientific	10569-044
Knockout DMEM	Life technology	10829-018
mTeSR1	Stem cell technologies	05850
Y-27632	Selleckchem	S1049
Definitive Endoderm kit	Stem cell technologies	05110
RPMI-1640	Life technology	61870-127
B-27 Serum free Supplement	Life technology	17504044
Penstrep 1×100	Life technology	15140163
Matrigel	Fisher Scientific	354277
FGF7	R&D Systems	251-KG-050
KAAD (KAAD-Cyclopamine)	Stemgent	04-0028
RA (All-Trans Retinoic Acid)	Stemgent	04-0021
LDN (LDN-193189)	Stemgent	04-0074-10
EGF	R&D Systems	236-EG-01M
Alk5i	Stemgent	04-0015
Zinc-sulfate (Zinc sulfate heptahydrate)	Sigma-Aldrich	Z0251-100G
Heparin	Sigma-Aldrich	H13149-10KU
T3 (3,3',5-Triiodo-L-thyronine)	Sigma-Aldrich	T6397-100MG
DBZ (γ-Secretase Inhibitor XX)	EMD Millipore	565789
N-Cys (N-Acetyl-L-cysteine)	Sigma-Aldrich	A9165-5G
Trolox	EMD Millipore	648471-500MG
R428	ApexBio	A8329

Supplemental Experimental Procedures

Generation of induced pluripotent stem cells and mutation correction by CRISPR/Cas9 system

Skin fibroblast cells were cultured in fibroblast culture media. iPSCs were generated from fibroblasts by manufacturers' instruction (SCR550, EMD Millipore) and a previously published protocol (Yoshioka et al., 2013). In brief, fibroblasts of 90% confluence were split one day before initiation of reprogramming onto four wells of a 12-well plate. Multiple wells with different splitting ratios were used to ensure at least one well was 80% confluent at the start of reprogramming. One day after splitting, cells were transfected for 1 day with VEE-OKS-iG mRNA expressing OCT4, KLF4, SOX2 and GLIS1, and B18R RNA by RiboJuice (TM) mRNA transfection kit (TR-1013, EMD Millipore). From day 2 to day 4, cells were treated with 0.05 μg/mL puromycin (A1113803, Gibco) to select for transfected cells and then allowed to recover without puromycin to 80% confluence from day 5 to day 8. On day 9, transfected fibroblasts were re-plated from one well of a 12-well plate to one well of a CF-1 IRR mouse embryonic fibroblasts (MEF) (A34181, Gibco) coated 6-well plate using MEF conditioned human embryonic stem cell (ESC)/induced pluripotent cell (iPSC) media with addition of 10 ng/ml bFGF (1791281B, Invitrogen), 1 μl/ml Human iPSC Reprogramming Boost Supplement II (SCM094, EMD Millipore) and 200 ng/mL B18R protein until the colonies began to form on day 16. From day 17 onward, cells were cultured with MEF conditioned human ES media with 10 ng/mL bFGF and 1 μl/mL Human iPSC Reprogramming Boost Supplement II until day 23 when individual colonies were picked and expanded. Patient iPSCs were karyotyped by G-band analysis by Cell Line Genetics.

Patient iPSCs with normal karyotypes were used for generating *INS* mutation corrected cells by Crispr/Cas9 system. gRNAs against *INS* gene locus close to the mutation were designed with the online tool (http://crispr.mit.edu/). gRNAs of 19 nucleotides (19 nt) long were cloned into vectors by PCR and Gibson assembly method. Human iPSCs were transfected with Cas9-GFP, guide RNA vectors and 198 nucleotide long single strand DNA (IDT, Integrated DNA Technologies) for mutation replacement by using human embryonic stem cell Nucleofector Kit (VVPH-5012, Lonza) and hESC medium supplemented with ROCK inhibitor (Y26732, Selleckchem) onto feeder cells. Fourty-eight hours post transfection, GFP positive cells were sorted by flow cytometry sorting machine (BD Influx Cell Sorter) and re-plated onto a 10-cm dish by using hESC medium with ROCK inhibitor. One day after sorting, change medium to normal hESC without Y26732 and after that change the same medium for every 2 days. After 2 weeks, individual clones were picked up and analyzed by Sanger sequencing for mutation correction events. PCR primers were listed in Supplemental Table 1.

Fibroblast culture medium consisted of DMEM-high glucose (10569-044, Gibco), 10% HyClone Fetal Bovine Serum (U.S.) (SH30088.03HI, GE Healthcare), and Pen Strep (15140-122, Gbico).
MEF conditioned human ESC/iPSC media were made with MEF conditioned media by adding 10 ng/mL bFGF, which was used only for generating iPSC.
Human ESC culture medium were made with KnockOut DMEM (10829018,Gibco), KnockOut Serum Replacement (10828028, Gibco), GlutaMAX Supplement (35050061, Gibco), MEM NEAA (11140050, Gibco), Pen Strep (15140-122, Gibco), 2-Mercaptoethanol (21985023, Thermo Fisher Scientific) supplemented with 0.01 μg/ml bFGF (1791281B, Invitrogen). Human

ESC culture medium was used for routinely culturing and passaging human pluripotent stem cells.

Flow cytometry analysis

Cells were dissociated to single cells and suspended in FACS buffer (PBS with 5 % FBS). First LIVE⁄DEAD stain diluted 1000 times in FACS buffer (Molecular Probes L34955, 1:1,000) was used to stain dissociated cells for 15 minutes in order to differentiating between live and dead cells during flow cytometry analysis. Then cells were fixed and permeabilized with Foxp3 staining buffer set (eBioscience) for 30 minutes. After fixed cells were washed twice with FACS buffer, they were incubated with primary antibodies for 30 to 60 minutes at 4℃. At last, cells were washed twice and stained with secondary antibodies for 30 to 60 minutes at 4℃. After finish staining, cell were analyzed by flow cytometer and gated along with isotype control samples only for live cells. All staining was performed at 4 degrees.

Primary antibodies used in the study are as follows: OCT4 (sc-8628, Santa Cruz biotechnology), SOX2(09-0024, Stemgent), anti-FOXA2 (3143S, Cell Signaling Technology), anti-SOX17 (AF1924, R&D Systems), anti-NKX6.1 (F55A10, Developmental Studies Hybridoma Bank), anti-PDX1 (AF2419, R&D Systems), anti-CHGA (MAB5268, Millipore), anti-MAFA (ab26405, Abcam), anti-C-peptide (GN-ID4, Developmental Studies Hybridoma Bank), anti-Glucagon (M182, Takara).
Second antibodies used in the study were listed as follows: Donkey Anti-Rat Alexa Fluor® 488 (712-545-153, Jackson Immuno Research Laboratories), Goat Anti-Rat Alexa Fluor® 555 (A-21434, Life Technologies), Donkey Anti-Rabbit Alexa Fluor® 555 (A-31572, Life Technologies), Donkey Anti-Rabbit Alexa Fluor® 488 (A-21206, Life Technologies), Donkey Anti-Guinea Pig Alexa Fluor® 647 (706-605-148, Jackson Immuno Research Laboratories), Donkey Anti-Goat Alexa Fluor® 555 (A-21432, Life Technologies), Donkey Anti-Goat Alexa Fluor® 488 (A-11055, Life Technologies), Donkey Anti-Mouse Alexa Fluor® 488 (A-21202, Life Technologies), Donkey Anti-Mouse Alexa Fluor® 555 (A-31570, Life Technologies). Information on Antibody dilution is provided in Supplemental table 2.

Insulin content and secretion analysis method

For insulin secretion assay, we treated live clusters with KRB medium for two hours. Clusters were first stimulated in 3.3 mM glucose and stimulated with 30.5 mM KCl for one hour respectively. After one hour of stimulation, supernatant was collected in order to measure insulin secretion by Mercodia Insulin ELISA kit (10-1113-01, Mercodia).
For insulin content, dissociated clusters were spun down and a total of 10^5 cells were sonicated in 50 µl water and mixed with acid ethanol (0.18 M HCl in 96% ethanol (v/v)) in a 1:3 proportion of sonicated product and acid ethanol. To extract insulin, the mixed sample was incubated at 4℃ for 12 hours. After that, acid ethanol extracts was stored at -70℃ or used for measuring insulin content with Mercodia Insulin ELISA kit (10-1113-01, Mercodia) .

KRB medium consisted of 128 mM NaCl, 5 mM KCl, 2.7 mM $CaCl_2$, 1.2mM $MgCl_2$, 1mM Na_2HPO_4, 1.2 mM KH_2PO_4, 5 mM $NAHCO_3$, 10 mM HEPES supplement with 0.1% BSA in deionized water, adjusted with NaOH to pH 7.4 and was sterilized by 0.22 µm filter (09-761-106, Fisher Scientific).

RNA analysis by RT-qPCR

RNA was extracted following the total RNA Purification Micro Kit (35300, Norgen Biotek) protocol. cDNA was generated from RNA by iScript Reverse Transcription Supermix (170-8841, Bio-Rad). RT-qPCR reaction system was setup by mixing cDNA and SsoFast EvaGreen Supermix (172-5202, Bio-Rad) and ran on the ABI thermal cycler (C1000 Touch Thermal Cycler). RT-qPCR primers were listed in Supplemental Table 1.

Transplantation and graft analysis methods

To transplant differentiated cells, around 200 clusters at day 27 of differentiation stage were suspended in 80 μl matrigel and transplanted into leg muscle of NSG mice (stock number 005557, The Jackson Laboratory). After three weeks post-transplantation, blood was collected from mouse tails, followed by subsequent collection every 2 weeks to analyze human C-peptide levels using a Mercodia Ultrasensitive C-peptide ELISA kit (10-1141-01, Mercodia). Daytime random measurements were performed. When human C-peptide reached up to 400 pmol/l or after19 weeks, mice were treated with STZ for amount of 150 mg/kg per mice (S0130-1G, Sigma Aldrich) to ablate mouse β cells in order to test whether transplanted human endocrine cells could help mice maintain normoglycemia. Mouse C-peptide was measured 7 days after STZ treatment with a Mouse C-Peptide ELISA Kit (90050, Crystal Chem) to make sure mouse C-peptide was eliminated before starting intraperitoneal glucose tolerance test (IPGTT). Mice had continuous access to food (standard diet).

IPGTT was performed 12 days after successful STZ treatment. For the IPGTT, mice were first fasted for 16 hours to keep them in a low blood glucose status. After fasting, an initial blood draw was done prior to each glucose challenge. For the glucose challenge, mice were injected intraperitoneally with 20% glucose of 10 times volume (μl) of body weight (g). Blood were drawn at 15, 30, 60 and 120 min after glucose injection. Glucose in the blood was measured by glucose meter (FreeStyle).

To monitor glucose dynamic homeostasis difference during day time and night, we performed 24 hour glucose measurement in 2 hour interval for STZ treated mice transplanted with corrected endocrine cells and WT mice by glucose meter (FreeStyle). Mice had continuous access to standard diet.

Supplemental References

Yoshioka, N., Gros, E., Li, H.R., Kumar, S., Deacon, D.C., Maron, C., Muotri, A.R., Chi, N.C., Fu, X.D., Yu, B.D., et al. (2013). Efficient generation of human iPSCs by a synthetic self-replicative RNA. Cell stem cell 13, 246-254.